Hindawi
Journal of Nanomaterials
Volume 2017, Article ID 8360823, 6 pages
https://doi.org/10.1155/2017/8360823

Research Article

Characterization of Ag-Doped p-Type SnO Thin Films Prepared by DC Magnetron Sputtering

Hoai Phuong Pham,[1] Thanh Giang Le Thuy,[1] Quang Trung Tran,[1] Hoang Hung Nguyen,[1] Huynh Tran My Hoa,[1] Hoang Thi Thu,[1] and Tran Viet Cuong[1,2]

[1]*Department of Solid State Physics, Faculty of Physics, University of Science, Vietnam National University, Ho Chi Minh City (VNU-HCM), 227 Nguyen Van Cu Street, District 5, Ho Chi Minh City, Vietnam*
[2]*LED Agri-Bio Fusion Technology Research Center, Chonbuk National University, Jeonju, Republic of Korea*

Correspondence should be addressed to Quang Trung Tran; tqtrung@hcmus.edu.vn and Tran Viet Cuong; tvcuong@hcmus.edu.vn

Received 24 August 2017; Revised 4 November 2017; Accepted 19 November 2017; Published 18 December 2017

Academic Editor: Mohamed Bououdina

Crystalline structure and optoelectrical properties of silver-doped tin monoxide thin films with different dopant concentrations prepared by DC magnetron sputtering are investigated. The X-ray diffraction patterns reveal that the tetragonal SnO phase exhibits preferred orientations along (101) and (110) planes. Our results indicate that replacing Sn^{2+} in the SnO lattice with Ag^{+} ions produces smaller-sized crystallites, which may lead to enhanced carrier scattering at grain boundaries. This causes a deterioration in the carrier mobility, even though the carrier concentration improves by two orders of magnitude due to doping. In addition, the Ag-doped SnO thin films show a p-type semiconductor behavior, with a direct optical gap and decreasing transmittance with increasing Ag dopant concentration.

1. Introduction

Among tin oxide compounds, tin dioxide (SnO_2) and tin monoxide (SnO) have attracted much attention due to their potential applications in optoelectronic devices such as solar cells, displays, sensors, and complementary oxide-thin film transistors [1–3]. The existence of different oxidation states in tin ion makes it more beneficial to have nonstoichiometric tin oxide phases. SnO_2 is generally an n-type semiconductor due to the existence of intrinsic defects such as oxygen deficiencies and tin interstitials; but, SnO exhibits p-type conductivity and relatively high hole mobility originated from the tin vacancy. From the literature concerned, most research work in the past has paid attention to SnO_2, whereas experimental reports on SnO are fewer because of its metastability and tendency to transform into SnO_2 at high oxygen pressures. However, interest in SnO has been recently resurged because of the difficulty in obtaining high quality p-type oxide semiconductor such as p-type-doped ZnO, NiO, and CuO. Several methods for preparation of p-type SnO thin films have been reported such as electron beam evaporation, pulse laser deposition, magnetron sputtering, and atomic layer deposition [4]. In these studies, postdeposition annealing was often necessary to improve the films crystallinity and obtain better p-type conductivity, but the resultant films displayed poor electronic transport properties. It is believed that the p-type conductivity of SnO can be further improved by proper doping. However, there are only a few literature reports on metal-doped SnO, and the doping effects thereof [5]. Guo et al. speculated that the increase in the concentration of Y doping in the SnO [6], the deterioration of crystallinity, and the increase in optical bandgap of SnO have been observed. Ahn et al. reported that increasing Mg doping concentration in SnO thin films results in lower crystallite size and higher resistance [7]. In this context, developing methods to produce p-type metal-doped SnO thin films are extremely needed. The successful preparation of this material may have a promising future in the next-generation transparent

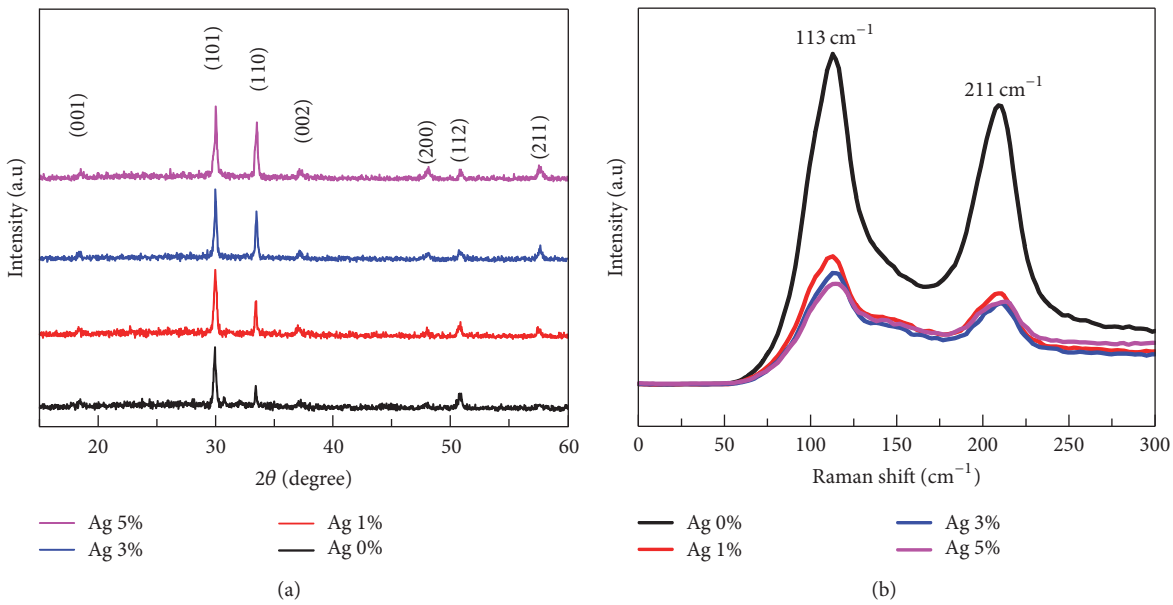

Figure 1: (a) XRD patterns and (b) Raman spectra of SnO thin films with different Ag dopant contents.

semiconducting oxide for application in novel optoelectronic devices. Herein, we investigate the crystallite structure and optoelectrical properties of Ag-doped SnO thin films directly deposited on glass substrates using DC magnetron sputtering system.

2. Experimental

SnO and Ag-doped SnO thin films were deposited on glass substrates using a DC magnetron sputtering system. Metallic Sn : Ag (1 at.%), Sn : Ag (3 at.%), and Sn : Ag (5 at.%) targets were prepared and used as the precursors for sputtering Ag-doped SnO thin films with different Ag contents. The glass substrates were immersed in 10% NaOH for 15 min, rinsed with a mixture of DI water, acetone, and ethanol (1 : 1 : 1) for 10 min, and blow-dried with N_2 gas before loading into the growth chamber. Ar and O_2 were used as the working gasses. The O_2 partial pressure was 12% at a working pressure of 5×10^{-3} Torr. Prior to growth, a 10-minute presputtering step was carried out in order to remove any contamination from the target surface. The DC power of the Ag-doped Sn targets was fixed at 24 W. The deposition time was kept at 25 min for all samples. Consequently, the SnO and Ag-doped SnO thin films exhibited a constant thickness of 500 nm, as measured using a stylus profilometer (Alpha Step D-600 Stylus Profiler). The surface morphology of the prepared samples was observed by scanning electron microscopy (SEM, S-4800 Hitachi) and atomic force microscopy (AFM, Nanocute, SII Nano Technology). The crystalline structure of the films was analyzed using a Labram 300 Raman measurement system (Horiba JOBIN YVON) and an X-ray diffractometer (XRD, D8-ADVANCE) operated at 40 kV and 40 mA with Cu–Kα radiation. The optical properties were investigated using a UV–VIS spectrometer (JASCO, V-550, Japan) and photoluminescence (PL) measurements. Hall measurements (HMS 3000) were carried out to measure carrier concentration and mobility at room temperature.

3. Results and Discussion

Figure 1(a) shows the XRD patterns of the undoped and Ag-doped SnO thin films with different Ag concentrations coated on glass substrates. The XRD patterns indicate that there are no impurity phases or other tin oxides such as SnO_2, Sn_3O_4, and Sn_2O_3 [8]. All samples were SnO with a tetragonal structure, indicating a strong (101) preferred orientation according to JCPDS card no 06-0395. With Ag doping, an increase in doping content causes a significant increase in the (110) diffraction peak intensity, which may be attributed to elongation of the tetragonal phase. Adding Ag did not change the crystal structure significantly. The full width at half maximum (FWHM) of the SnO (110) reflection peak was observed to increase from 3.07 to 4.92 corresponding to an increase of silver doping concentration from 0 to 5%. The average crystallite size, calculated from the Scherrer formula, decreases from 46.51 nm for the undoped SnO to 29.07 nm for the Ag-doped SnO (at. 5%). It indicated that the crystal size of the Ag-doped SnO films decreases with increasing dopant concentration and the FWHM must be inverse relation with the crystallite size. A feasible explanation for this observation is that the atomic radius of the Ag^+ ion (1.15 Å) is smaller than that of the Sn^{2+} ion (1.18 Å). Thus, exchanging Sn^{2+} for Ag^+ ions should reduce the crystal size. Raman spectroscopy is another powerful nondestructive technique for studying the microstructural properties of crystalline materials such as crystal quality, structure disorder, and defects in doped semiconductor alloys. It can provide

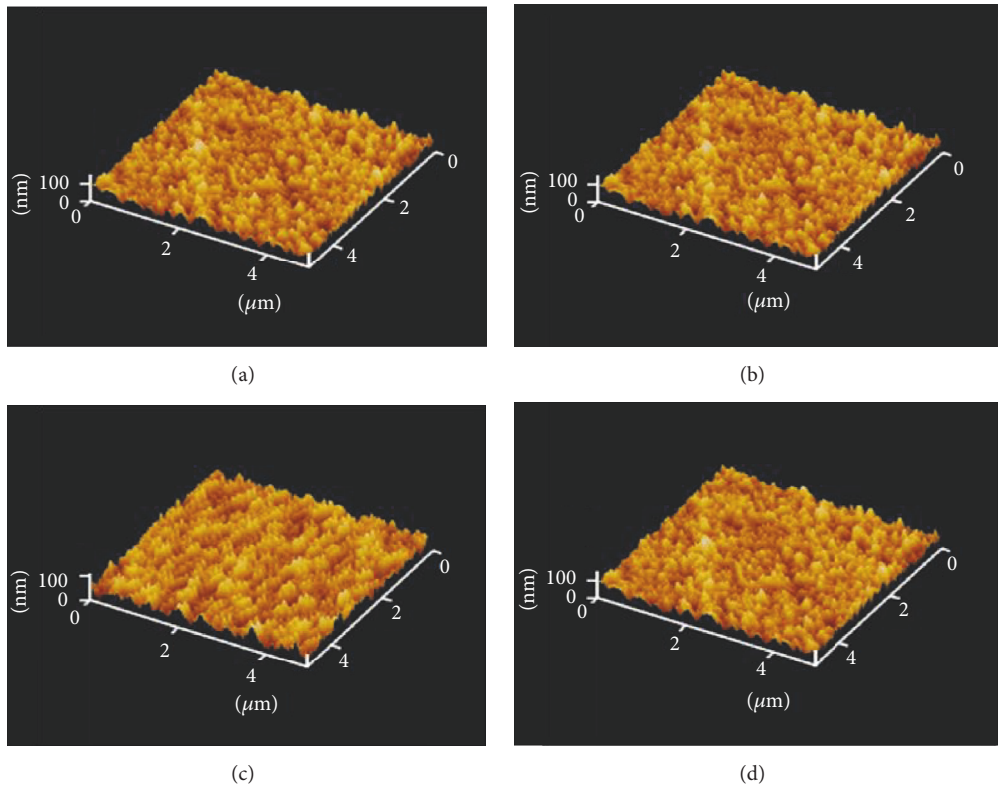

Figure 2: AFM images of SnO thin films with (a) 0 at.%, (b) 1 at.%, (c) 3 at.%, and (d) 5 at.% of the Ag dopant.

crucial information about local structural changes that arise due to the incorporation of Ag^+ ions into the SnO host lattice. As shown in Figure 1(b), the Raman spectra of the undoped and Ag-doped SnO thin films exhibit two Raman modes at 113 cm^{-1} (E_{1g}) and 211 cm^{-1} (A_{1g}), in excellent agreement with the theoretical and experimental values in the literature [9]. With increasing dopant concentration, the Raman spectra of the Ag-doped SnO samples exhibited a slight blue-shift, while the intensity of the above modes decreased dramatically. These trends, which were observed in this study for the first time, may possibly arise due to the incorporation of Ag^+ ions into the SnO host lattice, which affects lattice scattering, resulting in decreased peak intensity.

Figures 2(a)–2(d) show the AFM images of the undoped and Ag-doped SnO thin films with Ag concentrations of (a) 0%, (b) 1%, (c) 3%, and (d) 5%. The root-mean-square roughness (RMS) of these samples was approximately 11.9 nm, 12.6 nm, 14.5 nm, and 16.5 nm, respectively. Based on the XRD results (Figure 1), we inferred that the RMS of the films increases as a result of the reduction of the crystallite size when more Ag^+ ions are inserted into the SnO host lattice. This change leads to an increase in the number of grain boundaries, and thus increases the surface roughness. As seen in Figure 3, SEM images indicate that there was a slight increase in the number of grain boundaries, signifying a breakdown of the surface coalescence with increasing Ag dopant concentration. However, since all the samples were grown under identical growth conditions and on the same substrate, a similar microstructure and surface morphology was seen in all the SnO films. In other words, the XRD and AFM results were consistent with what was observed in the SEM images shown in Figure 3.

The core levels Sn(3d), O(1s), and Ag(3d) of XPS peaks for the undoped and Ag-doped SnO thin films with different concentration were demonstrated in Figures 4(a)–4(c). With silver doping, Figure 4(a) shows that the Sn $3d_{3/2}$ and Sn $3d_{5/2}$ binding energies moved approximately 0.3 and 0.17 eV toward a lower binding energy, respectively. Similarly, the Ag doping in SnO also led to a shift in the O1s spectrum toward lower binding energy approximately 0.2 eV. Decreasing the binding energy of the Sn(3d) and O(1s) levels with the increase in Ag doping could be due to the reduction of Sn-related defect and oxygen vacancy defects, but there was no change in the oxidation state of the tin in the SnO thin film. The chemical state of silver element was characterized by studying Ag(3d) levels as shown in Figure 4(c). The $Ag(3d_{5/2})$ and $Ag(3d_{3/2})$ peaks are located at the binding energy of 368.1 and 374.1 eV, respectively. These peaks were split to about 6 eV, indicating the formation of metallic silvers in the grown samples. Interestingly, it is clear to see that the peak intensity increases with silver dopant concentration. This observation is considered to be a solid evidence for enhancement of the substitution of Ag for Sn in SnO crystal lattice.

Figure 5(a) represents the PL spectra of the Ag-doped SnO thin films measured at room temperature using a He-Cd laser (λ = 325 nm). Generally, the visible peak located

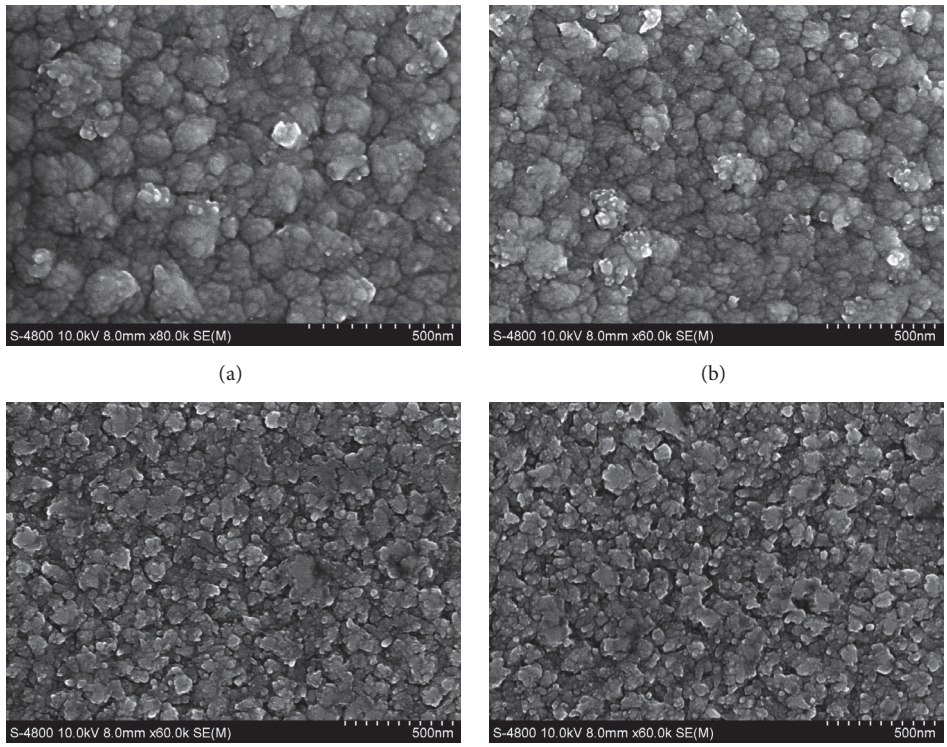

Figure 3: SEM images of SnO thin films with (a) 0 at.%, (b) 1 at.%, (c) 3 at.%, and (d) 5 at.% of the Ag dopant.

at 425 nm corresponds to the near band edge emission, and the broadband emission centered at approximately 530 nm is related to defects in SnO, which may arise from surface oxygen vacancies or tin interstitials formed during the substitution of Ag^+ for Sn^{2+} ions. We note that the band edge peak intensity decreases dramatically, while an obvious increase in the broadband emission is seen with increasing Ag dopant concentration. Taking this observation and XPS analysis into account, we suspect that introducing Ag^+ ions into the SnO host lattice, rather than the surface oxygen vacancies, acts as the dominant effect in determining the PL spectra. For further analysis of the optical properties, UV-Vis measurements were used to extrapolate the optical bandgap using Tauc's plots, that is, graphs of $(\alpha h\nu)^2$ versus photon energy ($h\nu$) [10]. As seen in Figure 5(b), the optical bandgaps of the Ag-doped SnO thin films were estimated to be approximately 2.7, 2.65, 2.63, and 2.6 eV for Ag dopant contents of 0%, 1%, 3%, and 5%, respectively. These values closely match the reported optical bandgap of tetragonal SnO (2.0–3.0 eV) [6, 7]. The optical bandgap of the SnO thin films tends to decrease with increasing dopant concentration. The decrease in the optical bandgap is thought to be attributed to the increase of the Ag_2O phase in the films because the optical bandgap of Ag_2O thin films is varied from 1.92~2.13 eV, lower than that of SnO. Moreover, we believe that many factors, including chemical composition, crystallite size, and the amount of structural defects could be responsible for the discrepancy between the optical bandgap values determined from PL and UV-Vis. The optical transmittance spectra of the undoped and Ag-doped SnO thin films are shown in the inset of Figure 5(b). The undoped sample shows an average optical transparency of 50% in the visible range. This value decreases to 40% in the 1% Ag-doped sample and to 30% in the 5% Ag-doped sample. In the case of noble metals like silver, the transmittance in the visible region is dominated by the absorption of light due to electronic transitions between occupied d states and unoccupied hybridized sp states above the Fermi level [11]. Therefore, the transmittance of the Ag-doped SnO thin films becomes lower at higher Ag dopant concentrations.

The electrical properties of the undoped and Ag-doped SnO thin films were investigated using Hall Effect measurements at room temperature utilizing the van der Pauw configuration. As seen in Figure 6, the Hall coefficient was a positive value, confirming the p-type semiconductor behavior of the Ag-doped SnO films. Figure 6 also shows the net hole concentrations, mobilities, and resistivities measured in the 500 nm thick Ag-doped SnO thin films with different dopant concentrations. Increasing the Ag dopant concentration causes the hole concentration to improve by nearly two orders of magnitude. However, the carrier mobility decreases dramatically, while the resistivity is unchanged. The unexpected result in terms of carrier mobility can be attributed to the degradation of film quality. Replacing Sn^{2+} ions with Ag^+ results in the formation of crystallites with a smaller size, which may lead to enhanced carrier scattering at grain boundaries, thereby deteriorating the carrier mobility.

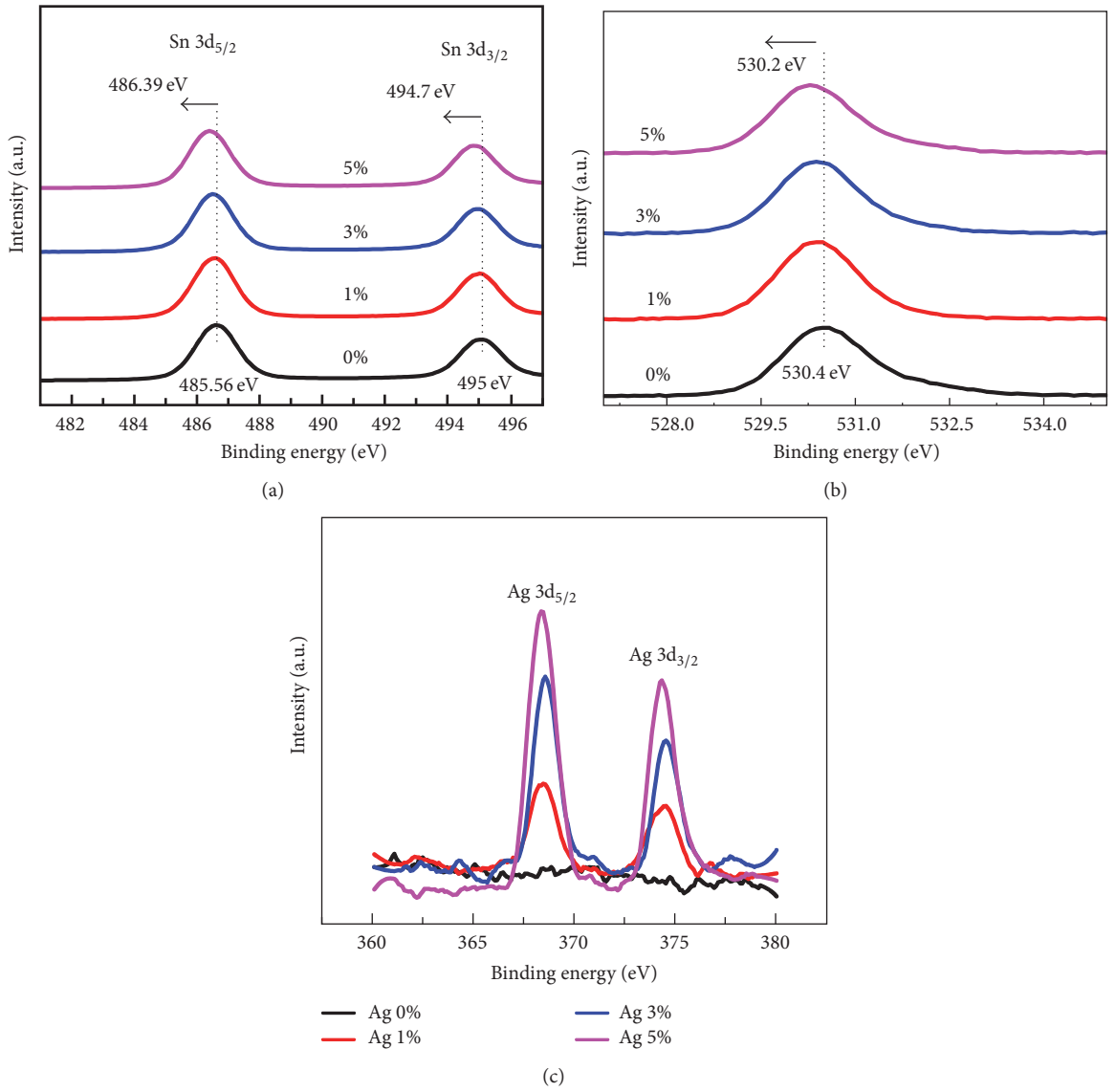

FIGURE 4: Survey XPS spectra of the Ag-doped SnO thin films: (a) Sn(3d) core level, (b) O(1s) core level, and (c) Ag(3d) core level, respectively.

4. Conclusions

Silver-doped tin monoxide thin films with different dopant concentrations were deposited on glass substrates using DC magnetron sputtering. After growth, their structural and optoelectrical properties were investigated. XRD analysis revealed that the resultant tetragonal SnO phase had preferred orientations along (101) and (110) planes. Upon increasing the Ag dopant concentration, Sn^{2+} ions were replaced with Ag^{+} ions, which results in a smaller crystallite size as confirmed by XRD and Raman spectra. By analyzing AFM and SEM images, we determined that the smaller crystallite size leads to an increase in the number of grain boundaries and a degradation of the surface coalescence, thereby increasing the surface roughness of the films. Consequently, the carrier mobility unexpectedly declined due to increased carrier scattering, even though the carrier concentration improved by two orders of magnitude in the doped films. In addition, optoelectrical characterizations revealed that Ag-doped SnO thin films exhibited a p-type semiconductor behavior, with a direct optical gap and decreasing transmittance as a function of increasing Ag dopant concentration.

Conflicts of Interest

The authors declare that they have no conflicts of interest.

Acknowledgments

This research was funded by the Vietnam National University, Ho Chi Minh City (VNU-HCM) under Grant no. C 2017-18-01 and also supported by the Basic Science Research Program through the National Research Foundation of

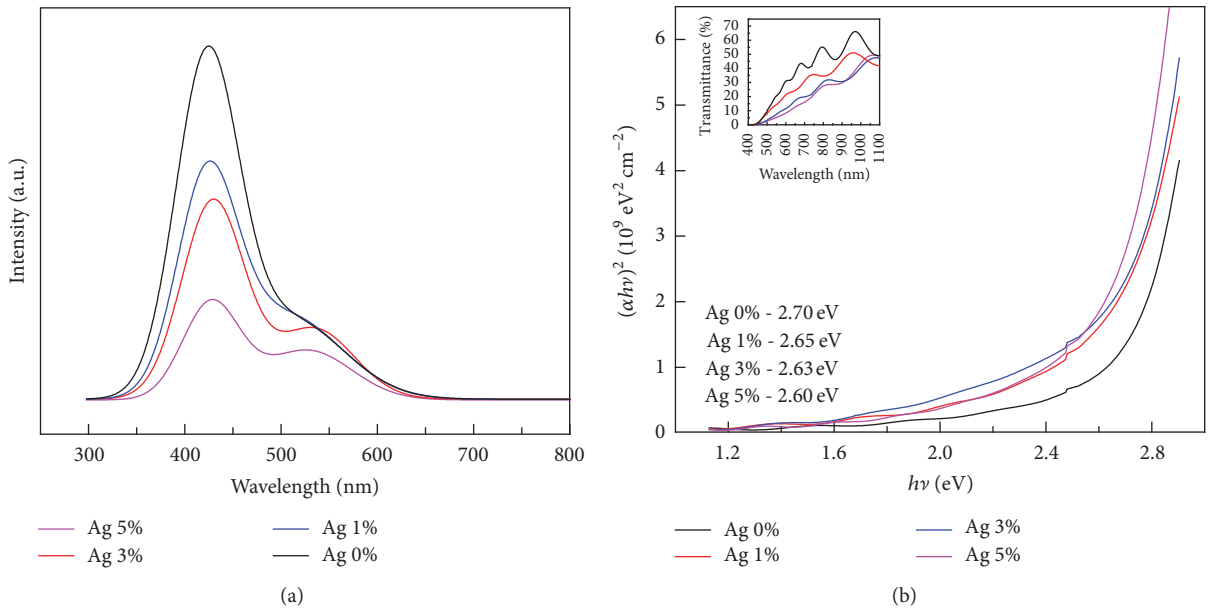

Figure 5: (a) Photoluminescence spectra and (b) Tauc's plots used to estimate the optical bandgap and transmission spectra (inset) of the Ag-doped SnO samples with different dopant concentrations.

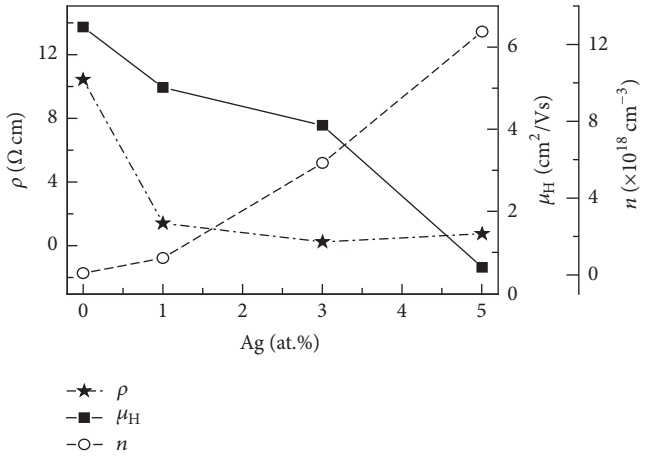

Figure 6: Plot of resistivity (ρ), carrier concentration (n), and Hall mobility (μ_H) versus Ag dopant concentrations in the SnO thin films.

Korea (NRF) funded by the Ministry of Education (NRF-2017R1D1A3B03030758).

References

[1] J. Watson, "The tin oxide gas sensor and its applications," *Sensors and Actuators*, vol. 5, no. 1, pp. 29–42, 1984.

[2] P.-C. Hsu, W.-C. Chen, Y.-T. Tsai et al., "Fabrication of p-type SnO thin-film transistors by sputtering with practical metal electrodes," *Japanese Journal of Applied Physics*, vol. 52, no. 5, Article ID 05DC07, 2013.

[3] L. Y. Liang, Z. M. Liu, H. T. Cao, and X. Q. Pan, "Microstructural, optical, and electrical properties of SnO thin films prepared on quartz via a two-step method," *ACS Applied Materials & Interfaces*, vol. 2, no. 4, pp. 1060–1065, 2010.

[4] H. Hosono, Y. Ogo, H. Yanagi, and T. Kamiya, "Bipolar conduction in SnO thin films," *Electrochemical and Solid-State Letters*, vol. 14, no. 1, pp. H13–H16, 2011.

[5] S. M. Ali, J. Muhammad, S. T. Hussain, S. A. Bakar, M. Ashraf, and Naeem-Ur-Rehman, "Study of microstructural, optical and electrical properties of Mg dopped SnO thin films," *Journal of Materials Science: Materials in Electronics*, vol. 24, no. 7, pp. 2432–2437, 2013.

[6] W. Guo, L. Fu, Y. Zhang et al., "Microstructure, optical, and electrical properties of p-type SnO thin films," *Applied Physics Letters*, vol. 96, no. 4, Article ID 042113, 2010.

[7] J. S. Ahn, R. Pode, and K. B. Lee, "Study of Cu-doped SnO thin films prepared by reactive co-sputtering with facing targets of Sn and Cu," *Thin Solid Films*, vol. 608, pp. 102–106, 2016.

[8] T. Yang, J. Zhao, X. Li et al., "Preparation and characterization of p-type transparent conducting SnO thin films," *Materials Letters*, vol. 139, pp. 39–41, 2015.

[9] Y. Q. Guo, R. Q. Tan, X. Li et al., "Shape-controlled growth and single-crystal XRD study of submillimeter-sized single crystals of SnO," *CrystEngComm*, vol. 13, no. 19, pp. 5677–5680, 2011.

[10] S. Das and T. L. Alford, "Structural and optical properties of Ag-doped copper oxide thin films on polyethylene napthalate substrate prepared by low temperature microwave annealing," *Journal of Applied Physics*, vol. 113, no. 24, Article ID 244905, 2013.

[11] A. Indluru and T. L. Alford, "Effect of Ag thickness on electrical transport and optical properties of indium tin oxide-Ag-indium tin oxide multilayers," *Journal of Applied Physics*, vol. 105, no. 12, Article ID 123528, 2009.